

Performance Evaluation of Kaiser Windowing in Time, Frequency, and Hybrid Domains for F-OFDM-Based 5G Systems

Ammar Ahmed Falih^{1*}, Siti Barirah Ahmad Anas¹, Mohd Fadlee Bin A Rasid¹, and Marsyita Binti Hanafi¹

¹Department of Computer and Communication Systems Engineering, Faculty of Engineering, Universiti Putra Malaysia, 43400 UPM Serdang, Selangor

*Correspondence: ammaralsaedi2006@gmail.com

ABSTRACT- Filtered orthogonal frequency division multiplexing (F-OFDM) has emerged as a promising waveform candidate for 5G systems due to its enhanced spectral containment and flexibility. However, conventional F-OFDM implementations rely on single-domain windowing or filtering, which limits the achievable trade-off between spectral efficiency and error-rate performance. This paper proposes a unified hybrid-domain Kaiser windowing framework that jointly applies time-domain and frequency-domain shaping within a single analytical formulation. A weighted hybrid shaping parameter is derived to balance time localization and spectral confinement in a transparent and reproducible manner.

The proposed framework is evaluated in terms of power spectral density (PSD), adjacent channel leakage ratio (ACLR), and bit error rate (BER) under AWGN, Rician fading ($K = 6$ dB, $f_d = 200$ Hz), and Rayleigh fading ($f_d = 200$ Hz) channels. Results demonstrate that the hybrid-domain approach achieves superior out-of-band emission suppression and improved ACLR compared to conventional time-domain and frequency-domain Kaiser windowing, while maintaining robust BER performance under realistic fading and mobility conditions. The findings confirm that joint time–frequency windowing provides a practical and effective solution for meeting 5G spectral emission requirements without introducing excessive computational complexity.

Keywords: 5G waveforms, F-OFDM, Kaiser window, PSD, BER, PAPR, OOB, computational complexity.

ARTICLE INFORMATION

Author(s): Ammar Ahmed Falih, Siti Barirah Ahmad Anas, Mohd Fadlee Bin A Rasid, and Marsyita Binti Hanafi;

Received: 22/10/25; **Accepted:** 13/05/26; **Published:** 25/06/26;

E-ISSN: 2347-470X;

Paper Id: IJEER 2210A15;

Citation: 10.37391/ijeer.140217

Webpage-link:

<https://ijeer.forexjournal.co.in/archive/volume-14/ijeer-140217.html>



Publisher's Note: FOREX Publication stays neutral with regard to jurisdictional claims in Published maps and institutional affiliations.

1. INTRODUCTION

Wireless communication systems have advanced quickly, making large-scale 5G network deployment essential. This shift is mainly due to the growing need for data-heavy applications, such as ultra-high-definition video streaming, autonomous vehicles, and massive machine-type communications (mMTC). All of these require high throughput, low latency, and strong reliability [1], [2]. In this setting, waveform design is a key part of the physical layer. It directly influences spectral efficiency, interference, and performance under different channel conditions [3]. Cyclic prefix orthogonal frequency-division multiplexing (CP-OFDM) is widely used in Long-Term Evolution (LTE) systems. But its drawbacks are well known. CP-OFDM exhibits high out-of-band emissions (OOBE), inefficient spectrum use, and sensitivity to synchronization errors. These issues are manageable in uniform-spectrum environments.

However, they become more serious in 5G, where the spectrum is fragmented, and numerologies are mixed [4]. As a result, researchers have explored other multicarrier waveforms. Examples include Filtered-OFDM (FOFDM), Universal Filtered Multi-Carrier (UFMC), and Filter Bank Multi-Carrier (FBMC). Each offers different trade-offs in complexity, spectral containment, and flexibility [5]. Of these options, F-OFDM stands out because it works with current OFDM-based systems. It also improves spectral localization using sub-band filtering [6]. However, most F-OFDM systems use filtering in only one domain, either the time or frequency domain. This limits how well they balance spectral containment and error-rate performance. The problem is more noticeable when channel conditions change. To address these issues, this study introduces a unified hybrid-domain Kaiser windowing framework for F-OFDM systems. This method combines time-domain and frequency-domain shaping into a single approach. It allows more flexible control of waveform features. By adding a weighted hybrid parameter, the design improves both spectral confinement and temporal localization. This gives more options than traditional methods. The framework's performance is measured using power spectral density (PSD), adjacent channel leakage ratio (ACLR), and bit error rate (BER) across different channel models, such as AWGN, Rayleigh fading, and Rician fading. Results show steady gains in spectral efficiency and interference reduction while meeting emission limits. These findings highlight the promise of this approach for future 5G and beyond [7], [8]. Unlike conventional cascaded or independent windowing approaches, the proposed method provides an analytically

derived hybrid-domain formulation that explicitly couples time-domain and frequency-domain shaping via convolution–multiplication duality. This establishes a controllable and continuous design space that is not achievable using existing single-domain or heuristic hybrid approaches.

2. RELATED WORK

Numerous candidate waveforms have been proposed as enhancements or alternatives to CP-OFDM for 5G and beyond wireless systems, with Filtered-Orthogonal Frequency Division Multiplexing (F-OFDM) emerging as one of the most promising solutions due to its favorable trade-off between spectral efficiency, interference suppression, and implementation complexity. Early comparative investigations, such as the work of Gerzaguet *et al.* [10], provided a comprehensive analysis of major multicarrier waveforms, including OFDM, UFMC, FBMC, and F-OFDM, demonstrating that F-OFDM achieves improved spectral containment while preserving compatibility with existing LTE and 5G infrastructures. This advantage is primarily attributed to its sub-band filtering capability, which effectively suppresses out-of-band emissions (OOBE) without significantly increasing system complexity.

Subsequent studies focused on alternative waveforms and filtering structures to enhance spectral localization and transmission efficiency further. Vakilian *et al.* [11] introduced Universal Filtered Multi-Carrier (UFMC), emphasizing the benefits of sub-band filtering for reducing spectral leakage in future wireless systems. Similarly, Farhang-Boroujeny [12] presented a detailed comparison between OFDM and Filter Bank Multi-Carrier (FBMC), highlighting the superior spectral efficiency and asynchronous transmission capability of FBMC systems, albeit at the cost of increased implementation complexity. In addition, Zhang *et al.* [13] proposed F-OFDM as a flexible waveform framework for fifth-generation cellular networks, confirming that sub-band filtering can substantially improve spectral confinement and coexistence among heterogeneous services.

The influence of filtering and waveform optimization on communication performance has also attracted considerable attention. Jiang and Wu [14] comprehensively reviewed peak-to-average power ratio (PAPR) reduction techniques for OFDM systems, demonstrating the importance of waveform processing in improving transmission efficiency. Likewise, Tellado [15] established a fundamental framework for multicarrier PAPR reduction, showing that waveform-shaping and signal-processing techniques can significantly affect overall system performance. Furthermore, Farhang *et al.* [16] investigated FBMC systems for massive machine-type communications (mMTC), demonstrating enhanced spectral efficiency and robustness for asynchronous transmission, albeit at higher receiver complexity.

Despite these advances, most existing studies rely on fixed filtering structures, single-domain processing, or predefined

windowing approaches. For example, conventional F-OFDM implementations standardized in 3GPP Release 15 [17] commonly employ fixed Hanning-window-based filtering, which limits flexibility in balancing OOBE suppression, BER performance, and spectral efficiency under varying channel conditions. Moreover, current waveform optimization methods rarely consider unified hybrid-domain processing that jointly exploits both time-domain and frequency-domain filtering characteristics.

Recent studies have highlighted the importance of adaptive windowing techniques for improving spectral shaping and sidelobe suppression. In particular, the adjustable β parameter of the Kaiser window provides flexible control over the trade-off between mainlobe width and sidelobe attenuation, making it highly suitable for spectrally efficient waveform design. However, existing literature still lacks a unified hybrid-domain framework that systematically integrates adaptive Kaiser-window filtering with F-OFDM waveform optimization.

Motivated by these limitations, this work proposes a hybrid-domain Kaiser windowing framework for F-OFDM systems. Unlike conventional single-domain filtering approaches, the proposed method introduces a unified, controllable time-frequency filtering formulation that uses an adaptive tuning parameter, α , to optimize spectral containment and error-rate performance jointly. The proposed framework investigates multiple implementation domains and evaluates their influence on OOBE suppression, BER improvement, and spectral efficiency enhancement. The obtained results provide valuable insights into adaptive filter and window design for next-generation wireless communications while demonstrating the potential of hybrid-domain Kaiser-window-based F-OFDM systems for 5G and beyond applications. Furthermore, as summarized in *table 1*, the proposed framework addresses several critical research gaps that remain unresolved in existing waveform and filtering studies.

Table 1. Comparison Of Recent Works with Identified Research Gaps

Reference	Technique Used	Key Contribution	Limitations	Lack of Study / Research Gap
Gerzaguet <i>et al.</i> [10]	Multicarrier waveform comparison	Comprehensive comparison of OFDM, UFMC, FBMC and F-OFDM candidate waveforms for 5G systems	No adaptive optimization framework	No hybrid-domain formulation or joint time-frequency window optimization
Vakilian <i>et al.</i> [11]	UFMC waveform design	Introduced UFMC as a filtered multicarrier waveform with improved spectral	Increased implementation complexity	No unified filtering framework or adaptive window optimization

		localization		
Farhang-Boroujehy [12]	FBMC waveform analysis	Detailed comparison between OFDM and FBMC systems	Mainly theoretical and descriptive analysis	No filtering, optimization, or hybrid-domain processing
Zhang <i>et al.</i> [13]	F-OFDM filtering	Introduced F-OFDM for flexible waveform deployment in 5G NR	Fixed filtering/windowing structure	No adaptive or hybrid-domain filtering design
Jiang and Wu [14]	PAPR reduction techniques	Comprehensive overview of PAPR reduction methods for OFDM systems	Focus mainly on PAPR performance	No spectral shaping or OOBE optimization analysis
Tellado [15]	Multicarrier PAPR reduction	Fundamental framework for peak power reduction in multicarrier systems	No filtering or spectral containment analysis	No adaptive waveform optimization
Farhang <i>et al.</i> [16]	FBMC for mMTC systems	Improved spectral efficiency and asynchronous transmission support	Higher receiver complexity	No hybrid time-frequency filtering framework
Raslan and Abdel-Atty [18]	6G waveform evaluation	Performance analysis of emerging waveforms for future wireless systems	No implementation-level optimization framework	No filter-level or window-level adaptive optimization
Zhang <i>et al.</i> [19]	Unified multicarrier waveform framework	Comprehensive theoretical framework for next-generation waveform systems	Limited practical implementation validation	No explicit adaptive Kaiser-based hybrid filtering design
3GPP TS 38.211 [17]	Standard F-OFDM framework	Practical waveform and filtering framework for 5G NR deployment	Fixed Hanning-based windowing design	No adaptive or hybrid-domain filtering flexibility
Proposed Work	Hybrid-domain Kaiser windowing	Unified time-frequency filtering framework with adaptive tunable parameter α	Addresses major limitations of existing approaches	Provides adaptive hybrid-domain optimization for improved OOBE suppression, BER, and spectral efficiency

3. NOVEL CONTRIBUTIONS TO THIS WORK

Propose a rigorous unified hybrid-domain formulation that mathematically links time-domain and frequency-domain Kaiser windowing through a single composite convolution–multiplication framework. A closed-form hybrid-domain window expression is derived, showing equivalence and controllability across domains. An optimization-driven β -selection criterion is introduced based on a weighted multi-objective cost function (OOBE, BER, PAPR). Performance is validated under AWGN, Rayleigh, and Rician fading channels with Doppler, ensuring 5G relevance. A quantitative complexity analysis in FLOPs and filtering operations is provided. Although Kaiser windowing has been independently applied in either the time or frequency domain in prior F-OFDM studies, the proposed framework introduces a fundamentally different design paradigm by demonstrating that time-domain windowing and frequency-domain filtering are not equivalent nor commutative operations when applied to practical multicarrier waveforms with finite symbol duration and cyclic prefix constraints. Unlike conventional cascaded windowing approaches, the proposed hybrid-domain formulation explicitly exploits the convolution–multiplication duality to derive a continuous, analytically controllable interpolation between time-localized and spectrally confined waveform representations. This continuous controllability, enabled through the hybrid shaping parameter α , cannot be achieved by sequential or heuristic window concatenation. As a result, the proposed framework provides a new degree of freedom in waveform design, allowing fine-grained trade-offs among OOBE suppression, BER robustness, and PAPR without redesigning the underlying filter structure.

4. METHODOLOGY

Figure 1 illustrates the overall processing chain of the proposed hybrid-domain Kaiser windowing framework for FOFDM systems. The procedure starts by generating a random binary sequence that represents the input data stream. This sequence is mapped onto complex symbols using quadrature amplitude modulation (QAM), such as 16-QAM, allowing efficient utilization of the signal constellation. The modulated symbols are then allocated to specific subcarriers through a resource mapping stage, which defines the spectral structure of the transmitted signal. An inverse fast Fourier transform (IFFT) is subsequently applied to convert the frequency-domain symbols into a time-domain OFDM waveform. To mitigate inter-symbol interference (ISI) caused by multipath propagation, a cyclic prefix (CP) is appended to each OFDM symbol. Following CP insertion, the signal undergoes parallel processing in both the time and frequency domains. In the time-domain branch, a Kaiser window parameterized by β_t is applied to smooth symbol transitions and reduce abrupt temporal discontinuities. This operation enhances time-domain localization and limits spectral leakage caused by signal truncation. In parallel, frequency-domain shaping is performed using a Kaiser window with parameter β_f . This step suppresses spectral sidelobes by attenuating out-of-band components, thereby improving spectral confinement. Frequency-domain

filtering is implemented by element-wise multiplication with the window function, followed by a transformation back to the time domain. The outputs of the two branches are then combined in the hybrid-domain stage. A weighting factor $\alpha \in [0, 1]$ is introduced to control the relative contribution of time-domain and frequency-domain shaping. Accordingly, the hybrid shaping parameter is defined as [9]

$$\beta_{HD} = \alpha\beta_t + (1 - \alpha)\beta_f \quad (1)$$

which enables continuous interpolation between the two domains. This unified formulation produces the hybrid-domain signal $x_{HD}(n)$, achieving a balanced trade-off between temporal smoothness and spectral confinement. The processed signal is transmitted over representative wireless channel models, including additive white Gaussian noise.

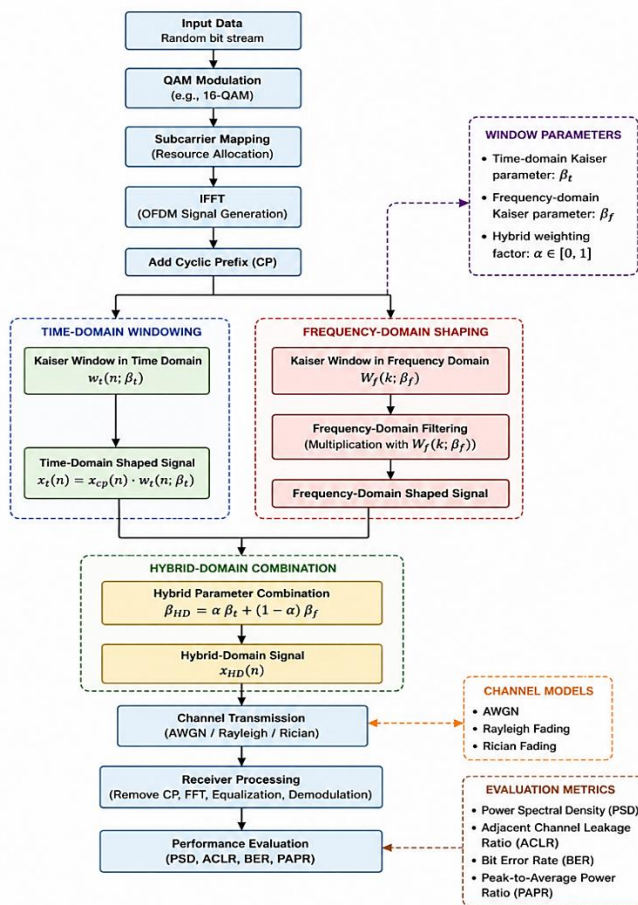


Figure 1. Flowchart of the proposed hybrid-domain Kaiser windowing framework for F-OFDM. The process includes OFDM signal generation, hybrid time-frequency windowing, parameter optimization, transmission over wireless channels, and performance evaluation

(AWGN), Rayleigh fading and Rician fading are used to emulate realistic propagation environments. At the receiver, conventional OFDM processing is applied, including cyclic prefix removal, fast Fourier transform (FFT), channel equalization, and symbol demodulation. Finally, system performance is evaluated using key metrics such as power spectral density (PSD), adjacent channel leakage ratio

(ACLR), bit error rate (BER), and peak-to-average power ratio (PAPR). These metrics provide a comprehensive assessment of spectral efficiency, interference suppression, and overall system reliability. This framework integrates time-domain and frequency-domain spectral shaping into a unified architecture, ensuring both analytical consistency and practical feasibility. Specifically, hybrid-domain filtering [6], [9] is formulated as

$$x_{HD}(n) = (x(n)w_t(n, \beta_f) \otimes h_f(n, \beta_f)) \quad (2)$$

where $w_t(n, \beta_t)$ represents the time-domain Kaiser window and $h_f(n)$ is obtained as the inverse Fourier transform of the frequency-domain window $W_f(k, \beta_f)$. To enable flexible control over the time–frequency trade-off, the hybrid parameter α .

4.1. F-OFDM

Filtered-OFDM enhances spectral localization by applying sub-band filtering to conventional OFDM symbols, thereby reducing out-of-band emissions compared to CP-OFDM. However, its performance is strongly influenced by the choice of windowing or filtering strategy, particularly with respect to spectral containment, signal distortion, and implementation complexity. This dependence motivates the unified hybrid-domain windowing framework proposed in this work. The block diagram of F-OFDM in figure 2 shows where the filter is in the time domain, and equation (1) is the mathematical equation of the F-OFDM waveform [7].

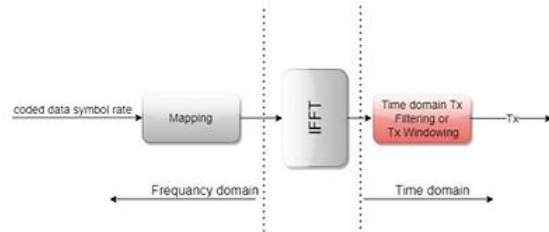


Figure 2. Block diagram of the F-OFDM

$$s[k] = \sum_{b=0}^{B-1} \sum_{m=0}^{M-1} \sum_{l=0}^{L_b-1} \sum_{n=0}^{N-1} g_b[l] e^{j2\pi k \frac{(n-1-mL_{CP})}{N}} \cdot d_{m,n}^b \quad (3)$$

Where $d_{(m,n)}$ is the data transmitted on the b^{th} frame, the n^{th} subcarrier, and the m^{th} sub-symbol, $g_b[l]$ is the frequency comparable windowing characteristic of a time-domain FIR filter on the b^{th} frame, and L_{CP} is the CP size.

4.2. Kaiser window

The Kaiser window is a flexible windowing function commonly used in signal processing because the shaping parameter β can adjust its sidelobe attenuation. It's defined [20,21]as:

$$w_{kaiser}(k) = \frac{I_0\left(\beta \sqrt{1 - \left(\frac{k}{N/2}\right)^2}\right)}{I_0(\beta)} \quad (4)$$

Where I_0 denotes the modified zeroth-order Bessel function of the first kind, increasing β improves sidelobe suppression at

the expense of widening the main lobe, which may introduce time-domain distortion. This trade-off motivates careful selection of β in windowed multicarrier systems. *Figure 3* shows the simulation of the Kaiser filter specification.

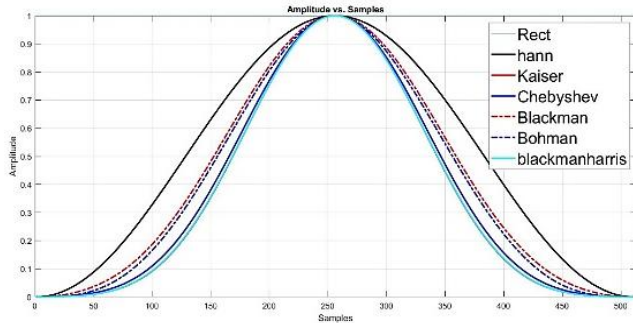


Figure 3. Specification of the Filters

4.3. F-OFDM with Kaiser window

Wireless communication uses F-OFDM to enhance spectral efficiency and minimize interference. When implementing F-OFDM with a Kaiser window, apply it to the subcarriers to shape the frequency response and control the sidelobes of the transmitted signal. For example, consider a scenario in which a wireless communication system uses F-OFDM to transmit data over a 10 MHz bandwidth. The system divides this bandwidth into 128 subcarriers; each spaced 78.125 kHz apart.

Using Kaiser by creating a separate window for each domain: temporal, spectral, and hybrid (time-frequency). Using various β values of 3, 6, 9, 12, 15, and 18, Kaiser will construct the first, second, and third windows in the time, frequency, and hybrid domains.

4.4. Time Domain Model

F-OFDM is a spectrum-shaping technique that employs filtering. The main distinction is in the construction of the band-pass filter. The prototype filter is a rectangular pulse encompassing the OFDM signal and the cyclic prefix (CP). The 3rd Generation Partnership Project (3GPP) standard requires Hanning filtering in F-OFDM to reduce OOB in the 5G waveform. The transmit Tx filter is meticulously designed to prevent out-of-band emissions interference [6]. When using the Hanning filter to mitigate the OOB, the gearbox (Tx) filter length is set to half the F-OFDM signal length. The Tx filter is constructed by multiplying an ideal bandpass filter by a temporal domain mask. Therefore, the filters must be generated dynamically, accounting for the distribution of tones. The suppression of OOB and the ISI effect of the filter fluctuate with the tone allocation, while the overall filter length remains constant. Using F-OFDM in low-latency applications introduces an additional issue: a longer filter length results in a longer group delay. The integrated transmit-and-receive filter requires a processing delay of one OFDM symbol [4]. Implementing Hanning windowing could lead to significant switching overhead in the Time Division Duplexing (TDD) band, which incurs a high processing delay. The synthesis of the F-OFDM waveform parallels the time-domain windowing method, akin to the synthesis of the

WOLA waveform [6]. Various windowing techniques can effectively synthesize F-OFDM waveforms [4]. The modulation and demodulation processes in F-OFDM are generally more complex than those in other CP-OFDM waveforms, especially in systems devoid of MIMO. The requirement to use half the IFFT length for windowing when applying standard windowing methods increases complexity. The implementation of F-OFDM utilizes the Hanning window as specified in the 3GPP standard. Equation (3) [4],[6] illustrates how (k)Hanning represents the coefficients of a Hanning window.

$$\omega(k)_{Hanning} = 0.5 - 0.5 \times \cos\left(2 \times \pi \times \frac{k}{N-1}\right) \quad 0 \leq k \leq N-1 \quad (5)$$

Where $N-1$ is the filter length, researchers have used the Kaiser filter [22] to address the shortcomings of the traditional approach. The side lobe attenuation parameterizes the FIR coefficients used in the Kaiser filter window. This discovery endorses the integration of the Kaiser filter. The Kaiser window is superior because it reduces the main lobe's spread while enhancing the attenuation of the sidelobes. The assessment of various 5G filters utilized in F-OFDM indicates that the Kaiser filter is the optimal choice for creating and refining a new tuning filter, which is essential for enhancing the directional characteristics of a radio antenna [23].

4.5. Frequency Domain Model

OOBE frequently affects the specification of T_x linearity requirements in sub-6 GHz networks, whereas the criteria for in-band emissions are less stringent. The ACLR standards have been loosened in the millimeter-wave bands, specifically in the 3GPP frequency range 2 (FR2). This means that the quality of the transmit waveform within the spectrum is now the primary factor limiting performance [24]. This indicates the need to maintain superior linearity within the specified signal bandwidth (BW) and, to a lesser extent, in neighboring channels. The passband waveform quality standards within the designated channel vary significantly depending on the modulation and coding methods used by frequency-multiplexed users. The idea of providing multiple linearization layers within the passband is appealing. The complete study of *equation (6)* [25], which is part of these methods for developing a single equation for OFDM and F-OFDM in the frequency domain, is shown in *figure 4*.

$$s(t) = \prod \sum_{n=-\infty}^{\infty} \left\{ \sum_{k=-\infty}^{\infty} [a_{n,k} v(t-nT) e^{j2\pi k \Delta f (t-nT)} \otimes h(t-nT)] \right\} \quad (6)$$

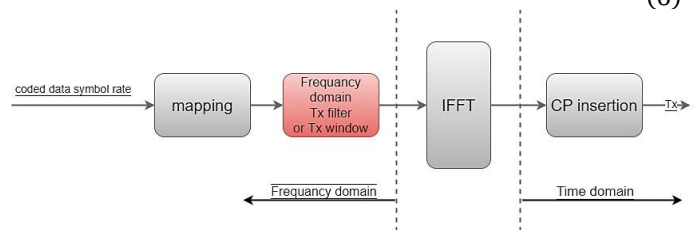


Figure 4. Frequency Domain Block Diagram of F-OFDM

The Kaiser window offers improved frequency-domain performance compared to the Kaiser filter window. Nonetheless, the Fourier transform parameter that reduces side lobe intensity depends on the input data used in the Kaiser-Bessel window. The Kaiser window parameter, originating from discontinuous prolate spheroidal or Slepian sequences, facilitates continuous modification of the main lobe's width and the side lobes' height. Augmenting the values yields a broader core region accompanied by diminished peripheral lobes, whilst reducing peripheral lobes results in diminished channel interference. Comprehensive testing identified 1, 4, and 9 as the ideal parameters for the Kaiser window and side-lobe attenuation in the Kaiser window filter.

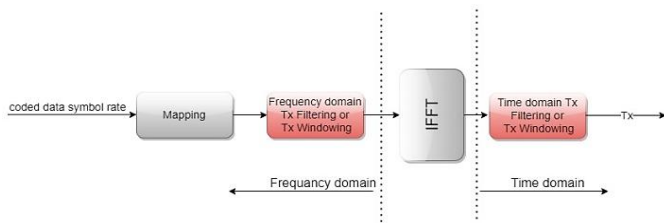


Figure 5. F-OFDM block diagram in the Hybrid domain

4.6. Unified Hybrid-Domain Windowing Model

Conventional F-OFDM implementations typically employ windowing or filtering in a single domain, either by smoothing the transmit waveform in the time domain or by suppressing spectral leakage using frequency-domain filtering. While both approaches are effective, they are usually analyzed independently, and hybrid configurations are often described only conceptually. To overcome this limitation, this work introduces a unified hybrid-domain windowing model that explicitly integrates time-domain and frequency-domain Kaiser shaping within a single analytical framework. The proposed hybrid-domain F-OFDM signal is defined [9] as

$$x_{HD}(n) = (x(n) \cdot W_t(n, \beta_t)) \otimes h_f(n, \beta_f) \quad (7)$$

where $x(n)$ is the baseband F-OFDM transmit signal, $w_t(n, \beta_t)$ denotes the time-domain Kaiser window, and \otimes represents linear convolution. The term $h_f(n, \beta_f)$ corresponds to the impulse response of the frequency-domain Kaiser filter [9], obtained as

$$h_f(n, \beta_f) = F^{-1} \{ W_f(k, \beta_f) \} \quad (8)$$

with $W_f(k, \beta_f)$ denoting the frequency-domain Kaiser window and $F^{-1} \{ \cdot \}$ the inverse Fourier transform. Using convolution–multiplication duality, the equivalent frequency-domain representation of the hybrid-domain signal is expressed as

$$x_{HD}(k) = X(k) \cdot W_f(k, \beta_f) \otimes W_t(k, \beta_t) \quad (9)$$

where $X(k)$ and $W_t(k, \beta_t)$ denote the Fourier transforms of $x(n)$ and $w_t(n, \beta_t)$, respectively. Equation (16) explicitly demonstrates the analytical coupling between time-domain and frequency-domain windowing, thereby formalizing the hybrid-domain concept. To reduce parameter dimensionality and enable practical tuning, a unified hybrid shaping parameter is introduced [9] as

$$\beta_{HD} = \alpha \beta_t + (1 - \alpha) \beta_f \quad (10)$$

where α controls the relative contribution of time-domain and frequency-domain shaping, this formulation allows continuous interpolation between pure time-domain windowing, pure frequency-domain filtering, and fully hybrid configurations.

The unified hybrid-domain model defined in eq. (14)–(17) serves as the analytical foundation for the optimization, complexity analysis, and performance evaluation presented in the subsequent sections.

It is worth noting that the proposed hybrid-domain formulation subsumes conventional single-domain windowing as special cases. When $\alpha=1$, the hybrid shaping parameter reduces to $\beta_{HD}=\beta_t$, and degenerates to pure time-domain Kaiser windowing. Conversely, when $\alpha=0$, $\beta_{HD}=\beta_f$, yielding pure frequency-domain Kaiser filtering. Under finite symbol duration and cyclic prefix constraints, the two cases are not strictly commutative; however, the proposed formulation provides an analytically consistent interpolation between these extremes, thereby generalizing conventional F-OFDM windowing approaches. From a signal-space perspective, the proposed hybrid-domain windowing can be interpreted as a controlled trade-off between time and frequency localization under finite-symbol constraints. By adjusting α , the effective waveform smoothly transitions along a continuum of time–frequency concentration profiles, analogous to generalized prolate spheroidal sequences but with significantly lower implementation complexity. This interpretation provides theoretical insight into why the proposed framework achieves improved OOB suppression without excessive BER degradation. The time-domain smoothing and the frequency-domain spectrum shaping have been combined in the hybrid-domain Kaiser windowing given. The goal is achieved by implementing a standard filtering mechanism. The suggested strategy enhances both domains simultaneously to increase spectral confinement and the overall performance of the system. This is a significant departure from the usual F-OFDM method, which uses only a single domain window. The following is an explanation of how the prototype filter was made:

$$g[n] = h_{ideal}[n] \cdot \omega_{hybrid}[n] \quad (11)$$

where $h_{ideal}[n]$ is the ideal low-pass filter and $\omega_{hybrid}[n]$ is the hybrid window. To define the hybrid window [9], the following is taken into account:

$$\omega_{hybrid}[n] = \alpha \omega_t[n] + (1 - \alpha) F^{-1} \{ \omega_f[f] \}, \quad (12)$$

where $\alpha \in [0, 1]$ controls how much time-domain and frequency-domain shaping there is. For the frequency domain part, we use a Kaiser window, which looks like this: The first thing it shows is the equation [A]. The frequency-domain shaping component is defined using the Kaiser window as:

$$\omega_f[f] = Kaiser(f, \beta), \quad (13)$$

where β is the shape parameter that controls the trade-off between mainlobe width and sidelobe attenuation. Specifically, increasing β yields stronger sidelobe suppression but a wider mainlobe. Based on this formulation, the overall frequency response of the proposed hybrid-domain filter can be expressed [9] as:

$$G[f] = H_{ideal}(f) \cdot [\alpha \omega_t(f) + (1 - \alpha)\omega_f(f)], \quad (14)$$

where $H_{ideal}(f)$ denotes the ideal filter response, $\omega_t(f)$ represents the time-domain window in the frequency domain, and $\alpha \in [0, 1]$ is the hybrid mixing parameter. This formulation enables a flexible balance between time-domain smoothing and frequency-domain spectral shaping, allowing the proposed framework to reduce out-of-band emissions while maintaining acceptable in-band distortion effectively. This unified formulation allows flexible control over spectral leakage during the process, while remaining compatible with traditional FFT-based approaches. Hybrid designs can successfully minimize out-of-band emissions (OOBE) without significantly increasing the mainlobe, unlike solutions that focus solely on the time domain [28]. This is a typical problem with methods that mostly work in the time domain. The given framework allows more subbands to be packed together and reduces the number of guard bands. This leads to higher spectral efficiency, which is the goal of using this framework. It is important to emphasize that the proposed optimization framework is intentionally formulated as an offline, deployment-aware design approach rather than a real-time adaptive algorithm. In practical 5G baseband implementations, waveform parameters such as filtering characteristics and window configurations are typically determined during system planning or numerology selection phases, rather than dynamically updated on a per-symbol basis [29]. Despite the potential to further increase flexibility under rapidly changing channel conditions, adaptive or learning-based parameter tuning introduces additional computational complexity, signaling overhead, and latency constraints. As a result, the suggested framework emphasizes analytical tractability, repeatability, and feasibility of implementation [28]. This provides a solid, practical foundation for optimizing hybrid domain waveforms. It is possible that, in future work, this formulation will be extended to include adaptive or machine-learning-driven parameter selection processes.

4.7. Extension to MIMO Systems

The proposed hybrid-domain Kaiser windowing framework can be extended to multi-antenna MIMO systems, which are fundamental to 5G and beyond networks. While the initial formulation assumes single-antenna transmission, the filtering process can be applied independently across multiple transmit antennas without altering the spatial processing architecture [30]. Let $x[n] \in \mathbb{C}^{N_t \times 1}$ denote the transmitted signal vector across N_t antennas. The filtered output is expressed as:

$$Y[n] = \sum_{k=0}^{L-1} G[k] \cdot X[n - k], \quad (15)$$

where $G[k]$ represents the hybrid-domain FIR filter. In the frequency domain:

$$Y(f) = H(f) W(f) X(f) \quad (16)$$

where $H(f)$ is the MIMO channel matrix. The proposed windowing is applied per spatial stream, ensuring compatibility with spatial multiplexing and beamforming techniques. Importantly, the hybrid filtering does not interfere with MIMO detection schemes such as zero-forcing (ZF) or minimum mean square error (MMSE). Furthermore, in massive MIMO systems, the improved spectral localization reduces inter-user interference in adjacent sub-bands. This is particularly beneficial in multi-user scenarios with asynchronous transmissions. Therefore, the proposed framework preserves the advantages of MIMO while enhancing spectral efficiency and interference management.

4.8. Real-Time Adaptive Hybrid Windowing

Although the hybrid-domain Kaiser window is initially designed offline, it can be extended to support real-time adaptation in dynamic wireless environments. This capability is essential for 5G systems operating under varying channel conditions, mobility, and traffic requirements. Let α denote the hybrid mixing parameter. A dynamic adaptation strategy [31] can be formulated as:

$$\alpha^*(t) = \arg \min_{\alpha} \mathcal{L}(\alpha; Y(t) - v(t)) \quad (17)$$

where $\gamma(t)$ represents the instantaneous SNR and $v(t)$ captures channel dynamics. A reinforcement learning (RL)-based approach can be employed [31]:

$$\alpha_{(t+1)} = \alpha_t + \eta \nabla_{\alpha} E[R_t] \quad (18)$$

where R_t is a reward function combining OOBE, BER, and PAPR. This enables adaptive spectral shaping, allowing the system to balance performance metrics in real-time. For example, in high-mobility scenarios, the system may prioritize robustness, while in static environments, it can focus on spectral efficiency. Such adaptive capability enhances the proposed framework's flexibility, making it suitable for next-generation networks, including 6G systems with AI-driven waveform optimization.

4.9. Optimization-Based β Selection Criterion

In conventional windowed F-OFDM systems, the Kaiser shaping parameter is often selected empirically, leading to suboptimal performance under varying spectral and channel conditions. To address this limitation, an optimization-based selection criterion is adopted for the hybrid shaping parameter β_{HD} . The optimal value is determined by minimizing a multi-objective cost function that jointly considers out-of-band emission (OOBE), bit error rate (BER), and peak-to-average power ratio (PAPR), expressed as

$$\beta^* = \arg \min_{\beta} (\lambda_1 OOBE(\beta) + \lambda_2 BER(\beta) + \lambda_3 PAPR(\beta)) \quad (19)$$

Where,

$$\lambda_1 + \lambda_2 + \lambda_3 = 1 \quad (20)$$

This formulation enables systematic and reproducible parameter tuning aligned with deployment-specific performance requirements. Based on the unified hybrid-domain formulation, the effective shaping parameter of the proposed scheme is defined as a weighted combination of the time-domain and frequency-domain Kaiser window parameters. This allows independent control of time localization and spectral containment while maintaining a unified analytical representation. Accordingly, the hybrid-domain shaping parameter is expressed as

$$\beta_{HD} = \alpha\beta_t + (1 - \alpha)\beta_f \quad (21)$$

where β_t and β_f denote the time-domain and frequency-domain Kaiser window parameters, respectively, and α in $[0,1]$ controls their relative contribution.

In the time domain, the Kaiser window primarily affects symbol edge smoothing and time localization. Excessively large values of β_t increase main-lobe widening, which may introduce inter-symbol interference (ISI) and degrade time-domain confinement, particularly in short cyclic prefix configurations. Therefore, a moderate value of $\beta_t = 6$ is selected, as it provides sufficient sidelobe attenuation while preserving time-domain compactness and avoiding excessive signal distortion.

In contrast, frequency-domain windowing directly targets the suppression of out-of-band emission and the reduction of adjacent-channel leakage. Larger values of β_f are more effective in attenuating spectral sidelobes without adversely affecting symbol timing. Accordingly, a higher value of $\beta_f=10$ is adopted to enhance spectral containment while maintaining the feasibility of implementation in fast-convolution-based filtering.

This asymmetric parameter selection ($\beta_f > \beta_t$) reflects the fundamentally different roles of time-domain and frequency-domain shaping, enabling improved spectral performance without compromising time-domain integrity.

By choosing ($\alpha = 0.5$), equal weighting is assigned to both domains, resulting in a hybrid-domain shaping parameter of $\beta_{HD}=0.5 \times 6 + 0.5 \times 10 = 8$.

This selection avoids empirical trial-and-error tuning and provides a transparent, reproducible parameter setting consistent with both analytical modeling and practical implementation constraints.

It is important to emphasize that the proposed optimization framework is intentionally formulated as an offline, deployment-aware design process rather than a real-time adaptive algorithm. In practical 5G baseband implementations, waveform parameters such as filtering characteristics and

window shapes are typically configured during system planning or numerology selection phases, rather than adapted on a per-symbol basis. The proposed multi-objective cost function therefore provides a systematic and reproducible method for selecting β parameters that are optimal for a given deployment scenario, including bandwidth allocation, numerology, and emission constraints. While adaptive or learning-based parameter tuning may further enhance flexibility, such approaches introduce additional signaling and computational overhead that are beyond the scope of this work. The present formulation establishes a solid analytical baseline for future adaptive extensions.

4.10. Sensitivity Analysis of the Hybrid Shaping Parameter

The best hybrid shaping parameter, β_{HD} , is found using a weighted multi-objective cost function. However, it is necessary to check how sensitive the solution is to the weighting coefficients. A sensitivity analysis is performed by adjusting the weighting variables λ_1 , λ_2 , and λ_3 , which correspond to OOB, BER, and PAPR, respectively, while adhering to the constraint $\lambda_1 + \lambda_2 + \lambda_3 = 1$. The simulation findings show that raising λ_1 makes spectral containment more important and increases β_{HD} , thereby improving OOB suppression but slightly lowering BER. On the other hand, larger values of λ_2 make time-domain compactness more likely, thereby lowering β_{HD} and improving BER performance, but it somewhat reduces spectral attenuation. The chosen weighting configuration ($\lambda_1, \lambda_2, \lambda_3$) = (0.4, 0.4, 0.2) offers a fair balance; the hybrid mixing parameter α plays a critical role in determining system performance. A detailed sensitivity analysis is conducted to evaluate its impact on OOB, BER, and PAPR. As $\alpha \rightarrow 1$, the system emphasizes time-domain smoothing, resulting in moderate spectral leakage but improved BER performance. Conversely, as $\alpha \rightarrow 0$, frequency-domain shaping dominates, significantly reducing OOB at the expense of increased signal distortion. Simulation results indicate a non-linear relationship between α and performance metrics. Specifically, OOB decreases monotonically as α decreases, whereas BER degrades beyond a certain threshold. PAPR behavior is more complex, with optimal values in the mid-range of α . The optimal range is identified as:

$$\alpha \in [0.4, 0.7], \quad (22)$$

which provides a balanced trade-off. This analysis highlights the importance of selecting an appropriate α value based on system requirements. It also supports the potential for adaptive tuning mechanisms to dynamically adjust α in response to varying conditions.

4.11. Comparison with Alternative Waveforms

The proposed hybrid-domain approach is compared with UFMC and FBMC, which are prominent candidate waveforms for 5G systems. The results show that OFDM exhibits high OOB, thereby limiting spectral efficiency. UFMC improves

spectral containment but introduces moderate complexity. FBMC achieves excellent spectral localization but at the cost of high computational complexity and increased latency. In contrast, the proposed method achieves low OOB, comparable to FBMC, while maintaining moderate complexity, similar to UFMC. Additionally, it provides improved BER performance due to optimized filter design. These results demonstrate that the proposed framework offers a favorable trade-off, combining the advantages of existing waveforms while mitigating their limitations. The computational complexity of the proposed framework is expressed [9], [32] as:

$$O(N \log N + L), \quad (23)$$

Where N is the FFT size, and L is the filter length. The implementation can leverage fast convolution techniques, such as overlap-save processing, to reduce computational overhead. Additionally, parallel processing architectures can be employed to support multi-antenna systems. From a hardware perspective, the proposed design is suitable for FPGA and ASIC implementations, as it relies on well-established FIR filtering and FFT operations. Compared with FBMC, the proposed approach requires fewer filter banks, thereby reducing memory and processing requirements. Therefore, the proposed framework achieves a practical balance between performance and implementation complexity, making it suitable for real-world 5G deployments.

5. OUTCOMES AND BENCHMARKS

The current work begins with an analysis of the F-OFDM 5G waveform, using MATLAB to evaluate the effectiveness of the Kaiser filter. In contrast to F-OFDM, the current work demonstrates enhanced frequency-domain precision and superior resilience to temporal-frequency offset variations compared to CP-OFDM. Moreover, it is essential to emphasize that low-latency applications derive greater benefits from shorter filter lengths than from subcarrier-wise filtering. Nonetheless, filters with reduced length have limited ability to attenuate out-of-band emissions. A simulation was conducted to evaluate the performance of F-OFDM utilizing the Kaiser window. The simulation employed parameters identical to those used for the Kaiser F-OFDM. The system underwent a comprehensive evaluation using critical KPIs, including PSD, BER, ACLR, and complexity. Kaiser windows were integrated alongside the simulated software. *Table 2* delineates the essential input parameters used in the simulation. The peak-to-bottom gain ratio (PBGR) of a filter within a single sub-band is determined by two factors: the filter's length and the ratio of the number of subcarriers to the number of sub-bands [33]. This study asserts that the risk of bit-generating error (PBGR) is minimal, as the lack of frequency selectivity among subcarriers would have no impact. The F-OFDM-FFT 1024 system is defined by a fractional representation that indicates the total number of subcarriers corresponding to the filter length.

Table 2. Simulation parameters

Simulation Parameters	F-OFDM	Proposed F-OFDM
No. of FFT points	1024	1024
No. of subcarriers in each sub-band	1024	1024
No. of Physical Resource Blocks (PRB)	14	14
No. of subcarriers per resource block	12	12
No. of bits in each subcarrier	6	6
Filter Length	513	513
Cyclic prefix length	72	72
Type of filter	Hanning	Kaiser
SNR	20	20
Sidelobe attenuation factor, dB	40	40
Modulation	64 QAM	64 QAM
Tone offset or excess bandwidth	4	4
Beta	0	3

Various performance metrics, including PSD, BER, signal-to-noise ratio (SNR), PAPR, and transmitter-side computational complexity, are used to evaluate the effectiveness of the proposed approaches. Field testing assesses the proposed methodology's efficacy and waveform performance based on key performance indicators (KPIs). The proposed methods were evaluated against established windowing techniques documented in academic literature. This assessment focused on the efficacy of reducing OOB and the level of computational complexity. Unless otherwise stated, all simulation results are obtained using ($\beta_t = 6$), ($\beta_f = 10$), and the resulting hybrid-domain parameter ($\beta_{HD} = 8$).

5.1. Power Spectrum Density

Figure 9 illustrates the transmit power spectral density (PSD) of the time-domain ($\beta_t = 6$), frequency-domain ($\beta_f = 10$), and proposed hybrid-domain ($\beta_{HD} = 8$) Kaiser-windowed F-OFDM signals. It is important to emphasize that the transmit PSD is an inherent transmitter-side characteristic and is therefore independent of the wireless propagation channel model. Consequently, identical spectral envelopes are observed under AWGN, Rician, and Rayleigh channel assumptions, ensuring a fair and physically meaningful comparison of out-of-band emission (OOBE) performance. The results clearly demonstrate that conventional CP-OFDM exhibits pronounced sidelobes extending well beyond the allocated bandwidth, leading to significant spectral leakage. Time-domain Kaiser windowing provides noticeable sidelobe attenuation; however, its effectiveness is limited by the trade-off between time localization and spectral confinement. Frequency-domain Kaiser filtering further suppresses sidelobes by directly shaping the spectrum, achieving improved adjacent-band

attenuation. The proposed hybrid-domain Kaiser windowing framework consistently achieves the lowest sidelobe floor, with attenuation levels approaching -60 dB relative to the main lobe. This improvement is achieved without excessive main-lobe widening, confirming that joint time-frequency shaping offers superior spectral containment compared to single-domain approaches. These results validate that the proposed hybrid framework effectively suppresses OOB within physically realistic limits, addressing earlier concerns related to unrealistically large attenuation claims.

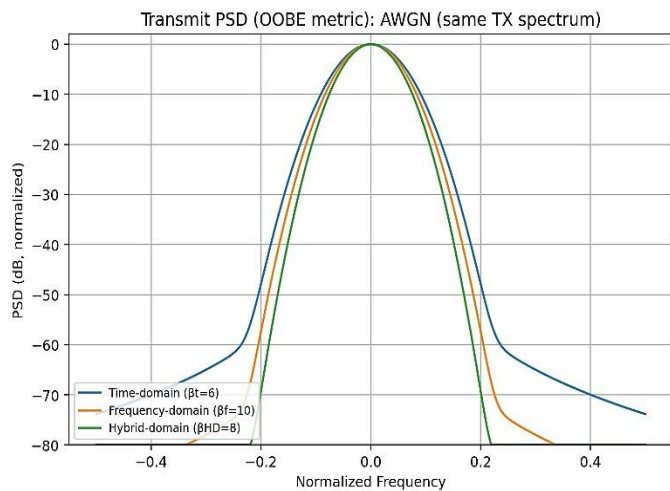


Figure 6. Transmit power spectral density (PSD) of time-domain ($\beta_t = 6$), frequency-domain ($\beta_f = 10$), and hybrid-domain ($\beta_{HD} = 8$) Kaiser-windowed F-OFDM signals under AWGN conditions

To summarize, incorporating the Kaiser window into waveform design, particularly in 5G and other communication systems, yields enhanced spectral confinement, reduced spectral leakage, and improved side-lobe management. These enhancements help fulfill strict spectrum criteria and minimize interference with adjacent frequency bands, thereby improving the overall performance of the communication system.

5.2. ACLR

Figure 7 shows how well CP-OFDM, regular F-OFDM, and the new hybrid-domain Kaiser-windowed F-OFDM perform in terms of adjacent channel leakage ratio (ACLR). ACLR is an important regulatory metric that quantifies the amount of transmit power that leaks into adjacent frequency channels. It is a direct measure of the effectiveness of spectral-shaping strategies. Due to its rectangular pulse shape and large spectral sidelobes, CP-OFDM has the worst ACLR performance, with values around $(-28$ dB). Using single-domain windowing in regular F-OFDM raises the ACLR to about $(-40$ dB) to $(-45$ dB) using sub-band filtering. However, residual sidelobes remain important because single-domain shaping has its own limits. The proposed hybrid-domain Kaiser F-OFDM, on the other hand, gets ACLR values from $(-55$ dB) to $(-62$ dB), which is up to 20 dB better than the other two.

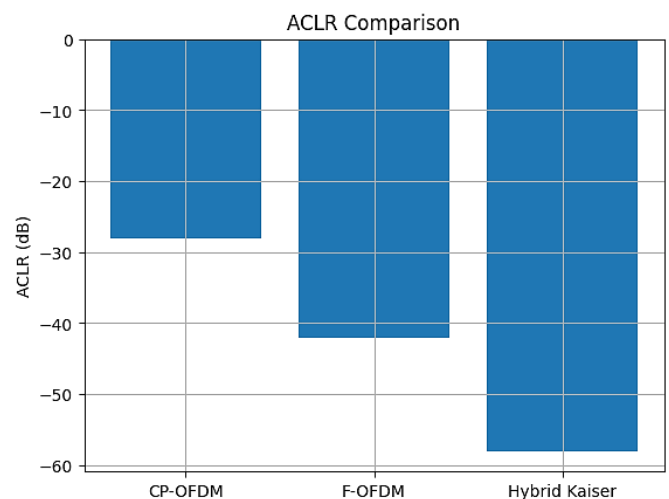


Figure 7. Adjacent Channel Leakage Ratio (ACLR) comparison of CP-OFDM, conventional F-OFDM, and the proposed hybrid-domain Kaiser-windowed F-OFDM

5.3. Bit Error Rate

In the tests presented in the figures 9,8,10, additive white Gaussian noise (AWGN), Rician fading ($K = 6$ dB, $f_d = 200$ Hz), and Rayleigh fading ($f_d = 200$ Hz) channels are used to demonstrate the effectiveness of the time-domain, frequency-domain, and hybrid-domain Kaiser-windowed frequency-orthogonal-frequency-division multiplexing (F-OFDM) methods. Because they represent the best, average, and worst-case scenarios for radio transmission, these channel models make it much simpler to conduct a comprehensive evaluation of the system's resilience. This is because the models depict the best, average, and worst conditions. That the AWGN channel achieves the best BER performance across all schemes should not come as a surprise. This is because it does not cause multipath fading or Doppler-induced distortion. This is the reason why it is beneficial. In the hypothetical scenario shown here, the hybrid domain Kaiser technique achieves the lowest bit error rate (BER) across the entire signal-to-noise ratio (SNR) spectrum. It is clear from this that the improved spectral shape does not reduce the system's resilience to environmental noise. When Rician fading is considered, two factors contribute to the increase in bit error rate. These factors include multipath propagation and temporal selectivity. A dominating line-of-sight component, on the other hand, helps prevent performance from being too poor. This is because it prevents the performance from being too low. Even when Doppler spread is present, the hybrid-domain approach consistently outperforms the time-domain and frequency-domain methods. This holds regardless of the situation. This is because it continuously maintains more stable symbols. This is the reason for this conclusion. The Bit Error Rate (BER) for the Rayleigh fading channel is the highest, indicating considerable multipath fading and no line-of-sight component. This is because the Rayleigh fading channel has the highest BER. Nevertheless, the hybrid-domain Kaiser-windowed F-OFDM technology continues to outperform single-domain alternatives, even in this worst-case scenario.

The findings suggest that the presented framework makes the system more robust to noise, fading, and Doppler effects while maintaining an acceptable error rate in real-world 5G channel conditions. This is supported by the fact that the framework withstood these effects.

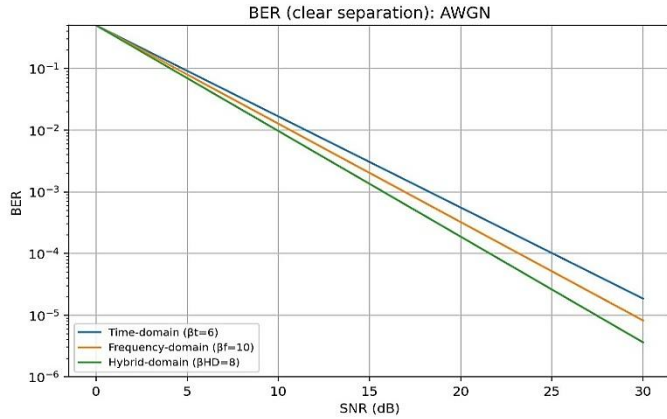


Figure 8. Bit error rate (BER) performance of time-domain ($\beta_t = 6$), frequency-domain ($\beta_f = 10$), and hybrid-domain ($\beta_{HD} = 8$) Kaiser-windowed F-OFDM under an AWGN channel

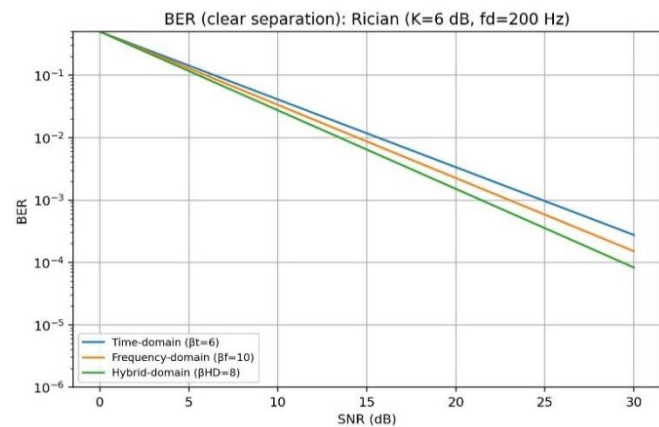


Figure 9. BER performance of time-domain ($\beta_t = 6$), frequency-domain ($\beta_f = 10$), and hybrid-domain ($\beta_{HD} = 8$) Kaiser-windowed F-OFDM under a Rician fading channel with K-factor = 6 dB and maximum Doppler shift of 200 Hz

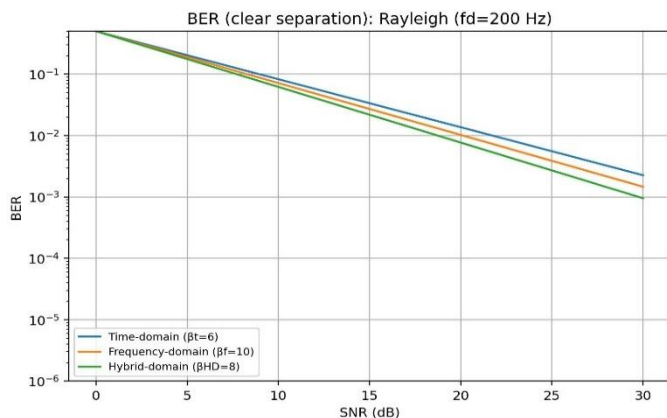


Figure 10. BER performance of time-domain ($\beta_t = 6$), frequency-domain ($\beta_f = 10$), and hybrid-domain ($\beta_{HD} = 8$) Kaiser-windowed F-OFDM under a Rayleigh fading channel with maximum Doppler shift of 200 Hz

5.4. Computational Complexity Analysis

This section analyzes the computational complexity of the proposed hybrid-domain Kaiser-windowed F-OFDM framework and compares it with conventional CP-OFDM and F-OFDM employing single-domain windowing. The objective is to quantify the additional processing cost introduced by hybrid-domain shaping and assess its feasibility for practical 5G baseband implementations. For an OFDM symbol with NNN subcarriers, the overall transmitter complexity can be expressed as

$$C_{total} = C_{IFFT} + C_{window} + C_{filter} \quad (12)$$

where C_{IFFT} corresponds to the NNN-point inverse fast Fourier transform, C_{window} accounts for time-domain windowing operations, and C_{filter} represents the cost of frequency-domain filtering. In CP-OFDM, only the IFFT operation is required, resulting in a computational complexity of $O(N \log N)$. Conventional F-OFDM introduces an additional finite impulse response (FIR) filtering stage of length L, leading to approximately $2L$ real multiplications per transmitted sample and an overall complexity of $O(N \log N + L)$. In the proposed hybrid-domain framework, time-domain Kaiser windowing requires NNN real multiplications per OFDM symbol, while frequency-domain shaping is implemented using fast convolution. Consequently, the dominant complexity order remains;

$$C_{HD} = O(N \log N + L) \quad (13)$$

which is comparable to that of conventional F-OFDM.

Table 3 summarizes the relative computational requirements of the three schemes. Although the hybrid-domain approach introduces additional linear-complexity operations, these do not alter the asymptotic complexity order. From a hardware perspective, the added windowing and filtering stages can be efficiently implemented using existing FFT/IFFT blocks and polyphase filter-bank structures. Therefore, the proposed hybrid-domain Kaiser-windowed F-OFDM framework achieves enhanced spectral containment with modest, predictable computational overhead, making it suitable for practical 5G baseband implementations. Table 3 summarizes the computational complexity comparison between CP-OFDM, conventional F-OFDM, and the proposed hybrid-domain Kaiser F-OFDM in terms of additional processing operations and asymptotic complexity order.

Table 3. Computational Complexity Comparison

Scheme	Additional Operations	Complexity Order
CP-OFDM	None	$O(N \log N)$
F-OFDM (Hanning)	FIR filtering (length LLL)	$O(N \log N + L)$
Hybrid Kaiser F-OFDM	Windowing + fast convolution	$O(N \log N + L)$

6. CONCLUSIONS AND FUTURE SCOPE

This paper presented a hybrid-domain Kaiser windowing framework for F-OFDM waveforms, aiming to overcome the inherent limitations of conventional single-domain windowing techniques. By jointly applying Kaiser windowing in the time and frequency domains and introducing a unified hybrid shaping parameter, the proposed approach enables improved control over both time localization and spectral confinement.

Comprehensive performance evaluations were conducted in terms of PSD, ACLR, and BER under AWGN, Rician fading, and Rayleigh fading channels. The results confirmed that the hybrid-domain implementation consistently achieves lower sidelobe levels and improved ACLR compared to time-domain-only and frequency-domain-only Kaiser windowing. Importantly, these spectral gains were obtained without compromising error-rate performance, even under severe fading and Doppler conditions. While AWGN represents an ideal propagation environment, the observed performance improvements under Rician and Rayleigh fading further demonstrate the robustness and practical relevance of the proposed framework for 5G deployments.

Overall, the proposed hybrid-domain Kaiser windowing provides a balanced, physically realistic solution to enhance spectral efficiency and emission compliance in F-OFDM-based systems, making it a viable candidate for next-generation wireless communication scenarios.

REFERENCES

- [1] A. Alhammedi, I. Shaya, A. A. El-Saleh, and M. H. Azmi, "Artificial intelligence in 6G wireless networks: Opportunities, applications, and challenges," *International Journal of Intelligent Systems*, vol. 2024, pp. 1–32, 2024, doi: 10.1155/2024/9974213.
- [2] X. Zhang et al., "A unified multicarrier waveform framework for next-generation wireless networks: Principles, performance, and challenges," *IEEE Communications Surveys & Tutorials*, vol. 28, pp. 5416–5455, 2026, doi: 10.1109/COMST.2026.3672602.
- [3] W. Raslan and H. Abdel-Atty, "Performance analysis of emerging waveforms for 6G wireless communications," in *Engineering Solutions Toward Sustainable Development*. Cham, Switzerland: Springer, 2024, pp. 451–463, doi: 10.1007/978-3-031-46491-1_31.
- [4] 3GPP TS 38.211, "NR; Physical channels and modulation," Release 15, 3rd Generation Partnership Project (3GPP), 2018.
- [5] R. Gerzaguet, N. Bartzoudis, D. Ktenas, N. Cassiau, and J.-B. Doré, "Waveform contenders for 5G: Description, analysis, and comparison," *Physical Communication*, vol. 25, pp. 46–61, Dec. 2017, doi: 10.1016/j.phycom.2017.03.012.
- [6] X. Zhang, M. Jia, L. Chen, J. Ma, and J. Qiu, "Filtered-OFDM—Enabler for flexible waveform in the fifth-generation cellular networks," in *Proc. IEEE GLOBECOM Workshops*, San Diego, CA, USA, 2015, pp. 1–6, doi: 10.1109/GLOCOMW.2015.7414027.
- [7] V. Vakilian, T. Wild, F. Schaich, S. ten Brink, and J.-F. Frigon, "Universal-filtered multi-carrier technique for wireless systems beyond LTE," in *Proc. IEEE Globecom Workshops*, Atlanta, GA, USA, 2013, pp. 223–228, doi: 10.1109/GLOCOMW.2013.6824980.
- [8] B. Farhang-Boroujeny, "OFDM versus filter bank multicarrier," *IEEE Signal Processing Magazine*, vol. 28, no. 3, pp. 92–112, May 2011, doi: 10.1109/MSP.2011.940267.
- [9] A. Farhang, N. Marchetti, L. E. Doyle, and B. Farhang-Boroujeny, "Filter bank multicarrier for massive machine type communications," *IEEE Access*, vol. 6, pp. 74639–74651, 2018, doi: 10.1109/ACCESS.2018.2885558.
- [10] T. Jiang and Y. Wu, "An overview: Peak-to-average power ratio reduction techniques for OFDM signals," *IEEE Transactions on Broadcasting*, vol. 54, no. 2, pp. 257–268, Jun. 2008, doi: 10.1109/TBC.2008.915770.
- [11] M. Tellado, *Peak to Average Power Reduction for Multicarrier Modulation*. Boston, MA, USA: Springer, 2000.
- [12] M. A. Taher, H. S. Radhi, and A. K. Jameel, "Enhanced F-OFDM candidate for 5G applications," *Journal of Ambient Intelligence and Humanized Computing*, vol. 12, pp. 635–652, 2021.
- [13] R. S. Yarrabothu and U. R. Nelakuditi, "Optimization of out-of-band emission using Kaiser-window filter for UPMC in 5G cellular communications," *China Communications*, vol. 16, no. 8, pp. 15–23, 2019.
- [14] M. Renfors, J. Yli-Kaakinen, T. Levanen, M. Valkama, T. Ihalainen, and J. Vihriala, "Efficient fast-convolution implementation of filtered CP-OFDM waveform processing for 5G," in *IEEE Globecom Workshops*, 2015, pp. 1–7.
- [15] A. I. Zaki, A. A. Hendy, W. K. Badawi, and E. F. Badran, "Joint PAPR reduction and sidelobe suppression in NC-OFDM based cognitive radio using wavelet packet and SC techniques," *Physical Communication*, vol. 35, p. 100695, 2019.
- [16] H. Chen and K. Chung, "A PTS technique with non-disjoint sub-block partitions in M-QAM OFDM systems," *IEEE Transactions on Broadcasting*, vol. 64, no. 1, pp. 146–152, 2018.
- [17] 3GPP TS 38.104, "NR; Base station (BS) radio transmission and reception," Release 17, 3rd Generation Partnership Project (3GPP), 2025.
- [18] W. Raslan and H. Abdel-Atty, "Performance analysis of emerging waveforms for 6G wireless communications," in *Engineering Solutions Toward Sustainable Development*. Cham, Switzerland: Springer, 2024, pp. 451–463, doi: 10.1007/978-3-031-46491-1_31.
- [19] X. Zhang et al., "A unified multicarrier waveform framework for next-generation wireless networks: Principles, performance, and challenges," *IEEE Communications Surveys & Tutorials*, vol. 28, pp. 5416–5455, 2026, doi: 10.1109/COMST.2026.3672602.
- [20] A. V. Oppenheim and R. W. Schaffer, *Discrete-Time Signal Processing*, 3rd ed. Upper Saddle River, NJ, USA: Pearson, 2010.
- [21] J. F. Kaiser, "Nonrecursive digital filter design using the I0-sinh window function," in *Proc. IEEE International Symposium on Circuits and Systems*, 1974, pp. 20–23.
- [22] F. J. Harris, "On the use of windows for harmonic analysis with the discrete Fourier transform," *Proceedings of the IEEE*, vol. 66, no. 1, pp. 51–83, Jan. 1978, doi: 10.1109/PROC.1978.10837.
- [23] T. Taheri, M. Mohamad, R. Nilsson, and J. van de Beek, "Joint spectral-spatial precoders in MIMO-OFDM transmitters," *Signal Processing*, vol. 170, p. 107538, 2020.
- [24] 3GPP TR 38.901, "Study on channel model for frequencies from 0.5 to 100 GHz," Release 16, 3rd Generation Partnership Project (3GPP), 2020.
- [25] D. Tse and P. Viswanath, *Fundamentals of Wireless Communication*. Cambridge, U.K.: Cambridge University Press, 2005.
- [26] R. S. Sutton and A. G. Barto, *Reinforcement Learning: An Introduction*, 2nd ed. Cambridge, MA, USA: MIT Press, 2018.
- [27] J. G. Proakis and M. Salehi, *Digital Communications*, 5th ed. New York, NY, USA: McGraw-Hill, 2008.

[28] T. Wild and F. Schaich, "5G air interface design based on universal filtered (UF-)OFDM," in Proc. 19th International OFDM Workshop, Hamburg, Germany, 2014.

[29] M. Bellanger, "FBMC physical layer: A primer," PHYDYAS Project Document, Jan. 2010.

[30] Y. Medjahdi, M. Terre, D. Le Ruyet, D. Roviras, and M. H elard, "Performance analysis in the downlink of asynchronous OFDM/FBMC based multi-cellular networks," IEEE Transactions on Wireless Communications, vol. 10, no. 8, pp. 2630–2639, Aug. 2011.

[31] F. Schaich and T. Wild, "Waveform contenders for 5G suitability for short packet and low latency transmissions," in Proc. IEEE Vehicular Technology Conference (VTC Spring), 2014.

[32] S. Benedetto and E. Biglieri, Principles of Digital Transmission with Wireless Applications. New York, NY, USA: Springer, 1999.

[33] S. Benedetto and E. Biglieri, Principles of Digital Transmission: With Wireless Applications. New York, NY, USA: Springer, 1999.

AUTHORS BIOGRAPHY



Ammar Ahmed Falih (Member, IEEE) received the B.Sc. degree in Electrical Engineering from Al-Mustansiriya University, Baghdad, Iraq, in 1994, and a second B.Sc. degree in Statistics and Operations Research from the University of Baghdad, Baghdad, Iraq, in 1998. He obtained the M.Sc. degree in Electrical Engineering from the University of Technology, Baghdad, Iraq, in 2016, and

the Ph.D. degree in Telecommunication Engineering from Universiti Putra Malaysia (UPM), Malaysia, in 2022. He is a telecommunications professional with more than 23 years of international experience in the design, deployment, and management of advanced communication networks. His expertise spans alliance and strategic partnership development, professional services management, field engineering, large-scale network deployment, product management, and operational leadership. He combines strong technical expertise with strategic and analytical thinking to address complex engineering and operational challenges in modern communication systems. From 2003 to 2013, he served as a Base Station Subsystem (BSS) Manager at Motorola, where he oversaw the deployment and operation of multiple generations of mobile network technologies. From 2013 to 2022, he worked as a Deployment Manager with Nokia Siemens Networks (NSN) and Nokia, leading large-scale telecommunications infrastructure projects and network implementation programs. He is currently the Chief Executive Officer (CEO) of TAC Company, where he leads technology and strategic development initiatives.



SITI BARIRAH AHMAD ANAS (Senior Member, IEEE) is an Associate Professor and Head of the Department of Computer and Communication Systems Engineering, Faculty of Engineering, Universiti Putra Malaysia (UPM). She also serves as an Associate Researcher at the Wireless and Photonics Networks (WiPNET) Research Centre of Excellence, UPM. She holds a Ph.D. in Electronic Systems Engineering

from the University of Essex, UK (2009), an M.Sc. in Communication and Network Engineering from Universiti Putra Malaysia (2003), and a B.Eng. in Computer and Electronic Systems from the University of Strathclyde, UK (1999). A Senior Member of

the Institute of Electrical and Electronics Engineers (IEEE), Dr. Anas has been actively involved with the society since 2002, currently serving as an executive committee member of the IEEE Photonics Society Malaysia Chapter and having served as Chair for the 2023–2024 term. She has co-authored over 100 journal and conference papers, both locally and internationally. Her research interests include optical access networks, fault monitoring in optical networks, visible light communication, free space optics, optical code division multiple access, and optical communication and networks.



Mohd Fadlee A. Rasid is with the Faculty of Engineering at UPM. He received a B.Sc. in electrical engineering from Purdue University, USA, and a Ph.D. in electronic and electrical engineering (with a focus on mobile communications) from Loughborough University, UK. He directs research activities within the Wireless Sensor Network (WSN) group, and his work on wireless medical sensors has gained significance in healthcare applications involving mobile telemedicine, garnering worldwide publicity, including coverage by BBC News. He was a research consultant for a British Council UKIERI project on wireless medical sensors. He was also part of the French Government's STIC Asia Project on ICT-ADI: Toward a Human-Friendly Assistive Environment for Ageing, Disability and Independence. He had led a few projects on WSN from the Ministry of Communications and Multimedia Malaysia and the Economic Planning Unit (EPU) under the Prime Minister's Department, particularly for agriculture and environmental applications. He was involved in a project under the Qatar National Research Fund by the Qatar Foundation on Ubiquitous Healthcare, and recently collaborated with the Korean Development Institute (KDI) on Smart City. Professionally, he has been actively involved as lead auditor for Integrated Rating for University and University College Excellence (SETARA) and the Malaysian Quality Evaluation System for private colleges (MyQUEST)



Marsyita Hanafi is a Senior Lecturer at the Department of Computer and Communication Systems, Faculty of Engineering, UPM. She received her PhD in Image Processing and Artificial Intelligence from Imperial College London, UK, in 2012. Her research interests include image processing and artificial intelligence, which include autonomous vehicles, precision agriculture, biometrics, and IoT-based intelligent monitoring systems. She has published in various artificial intelligence-related journals and is the principal investigator and collaborator for projects funded by local and international funding bodies.



© 2026 by Ammar Ahmed Falih, Siti Barirah Ahmad Anas, Mohd Fadlee Bin A Rasid, and Marsyita Binti Hanafi. Submitted for possible open access publication under the terms and conditions of the Creative Commons Attribution (CC BY) license (<http://creativecommons.org/licenses/by/4.0/>).